International Journal of Pure and Applied Mathematics
Volume 119 No. 14 2018, 1509-1519
ISSN: 1314-3395 (on-line version)
url: http://www.ijpam.eu
Special Issue
ijpam.eu

RECOGNITION OF DIABETIC RETINOPATHY USING SALIENT FEATURES OF DIGITAL FUNDUS IMAGE

L.M. Varalakshmi[1], R. Kurinjimalar[2] and K.Vijayakumar[3]
[1,2,3]Department of ECE, SMVC, Pondicherry, India

ABSTRACT:

Diabetic Retinopathy syndrome is a major cause of preventable optical incapacitation in the world. It is a complication of diabetes which can additionally affect sundry components of the body. When the minuscule blood vessels have a high caliber of glucose in the retina, the vision will be blurred and can cause visual impairment eventually. This is kenned as diabetic retinopathy. Customary screening is essential in order to detect the early stages of diabetic retinopathy for timely treatment to avert or delay further deterioration. This project detects the presence of abnormalities in the retina such as the structure of blood vessels, microaneurysms, exudates and texture properties utilizing image processing techniques. These features are input for automatic detection and can expeditiously process an immensely colossal number of fundus images obtained from mass screening to avail reduced cost and increment productivity and efficiency for ophthalmologists.

INTRODUCTION

Diabetic Retinopathy causes progressive damage to the retina, the light-sensitive lining at the back of the ocular perceiver. Diabetic retinopathy is an earnest visual perception-threatening complication of diabetes. Diabetes interferes with the body's competency to utilize and store sugar (glucose). The disease is characterized by an extravagant amount of sugar in the blood, which can cause damage throughout the body, including the ocular perceivers.

When people with diabetes undergoes ages of high blood sugar, fluid can accumulate in the lens of eye. This transmutes the curvature of the lens, foremost to blurred vision. However, once blood sugar levels are controlled, blurred distance vision will upgrade. Patients with diabetes who can render the blood sugar levels will inactive the progression of diabetic retinopathy.

The prior stages of diabetic retinopathy have no symptoms. Early detection and treatment can constrain the potential for consequential vision loss from diabetic retinopathy. Treatment of diabetic retinopathy varies by the situation of the disease. Diabetic retinopathy need laser surgery to heal leaking blood vessel. People with Chronic cases of diabetic retinopathy may need a surgery to remove the undesirable features from the eye.

Robust screening methods increases the accessibility of ocular perceiver care providers with timely intervention to avert the vision loss caused by diabetic retinopathy (DR) [1]. Digital color fundus photography has become a prerequisite for automated DR detection due to its patient amicableness and cost efficacy [2]. Recently a study by International Diabetes Federation found diabetes will optically discern an epidemic magnification closing to 552 million people by 2030 [3]. Besides this complications arising from diabetes are additionally growing including DR, which is the root cause of optical incapacitation within the 20–74 age group in most of the developed countries and presently affect 2–4% of diabetic people [4]-[6].

The most prevalent designations of DR are red lesions (microaneurysms, hemorrhages) and effulgent lesions (exudates, drusen and cotton wool spots). The presence of red lesions and/or hard exudates (effulgent lesions) are indicative of early stage DR. Microaneurysms (MAs) are focal dilatations of retinal capillaries and appear as red dots in retinal fundus images. Effulgent lesions or intraretinal lipid exudates results from the breakdown of blood retinal barrier. Omitted fluid affluent in lipids and proteins leave the parenchyma, leads to retinal edema and exudation. Lastly, wherever capillary walls are impuissant inside the retina, dot hemorrhages lesions are found which are marginally more sizably voluminous than MAs. On rupturing it will cause intra-retinal hemorrhages. Progression of DR additionally causes macular edema, neo-vascularization and in later stages, retinal detachment which is called Non-Proliferative Diabetic Retinopathy(NPDR). The Proliferative (PDR) and Non- Proliferative Diabetic Retinopathy are depicted in Fig. 1 with main retinal structures highlighted.

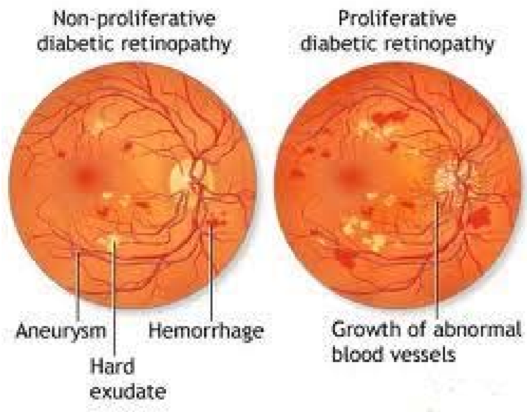

Fig.1 NPDR and PDR

1. RELATED WORKS

Systematic screening by ocular perceiver care specialists of diabetic patients is a cost-efficacious health care practice that can diagnose the pathology at the initial stage [7], [8]. In order to accommodate the screening and annual review requisite of an immensely colossal number of patients, an automated screening implements an utilizable adjunct in diabetes clinics. At present, there are several methods which can accurately diagnose concrete DR cognate lesions [9]–[11].

A different method is described in [12] that apply image structure clustering to cluster some replication vectors, to engender by a filterbank, and to find the most consequential set of structures in quality images. These structures are learned from a supervised method used to relegate incipient fundus images. Another approach category found in the literature probes for generic image parameters such as focus, color, illumination, and contrast. [13] present an algorithm that calculates each parameter discretely and then utilizes a classifier to relegate fundus images as gradable or ungradable. In [14], the authors compared the methods that use generic parameters (statistical feature) and methods that segment anatomical retinal structures (vessel features). Several studies present the coalescence of structural parameters with generic parameters in their systems [15], [16].

Diabetic retinopathy which is considered as the critical disease with deference to ocular perceiver can significantly result in visual impairment by 50%. Optimally Adjusted Morphological Operator (OCT) [17] investigated the states of the patients and presented optimally adjusted morphological operators for efficient detection of exudates. One of the main drawbacks of this method was that these detected exudates do not have detailed feature selecting technique for diabetic retinopathy detection. A detection framework was proposed for choroidal neovascularization (CNV) featured by leakage. However, detection of CNV involves analysis of a diminutive area of the retina only other than the entire image. [19] And [20] applied AdaBoost methods to relegate the leakage regions of FA images predicated on multiple handcrafted features. However, these supervised methods are circumscribed by their dependence on training datasets derived from manual annotation. The performance of the classifier will be inherently dependent on the quality of this annotation.

2. PROPOSED WORK

The proposed method utilizes three database of diabetic retinopathy and they are Diaretdb1, Messidor and Retinopathy Online Challenge (ROC).

Table 1: Details of Database

DATABASE	NUMBER OF IMAGE SAMPLES	IMAGE FORMAT
DIARETDB	89	JPEG
MESSIDOR	100	TIFF
ROC	50	PNG

(a) Image Acquisition

The Diaretdb1 database composed of 89 colour fundus images in which 84 belong to least mild non-proliferative signs (Microaneurysms) of the diabetic retinopathy, and 5 are intended as normal symptoms of diabetic retinopathy according to all experts who associate with the evaluation. The images were taken using the same 50 degree field-of-view digital fundus camera by varying imaging settings.

The Messidor database the 1200 retinal fundus color numerical images of the posterior pole for the Messidor database were captured by 3 ophthalmologic departments utilizing a color video 3CCD camera on a Topcon TRC NW6 non-mydriatic retinograph with a 45 degree field of view. The images were captured by acquiring 8 bits per color plane at 1440*960, 2240*1488 or 2304*1536 pixels in TIFF format.

The ROC database aids the patients with diabetes by means of computer aided detection and diagnosis (CAD) of diabetic retinopathy. Diabetic retinopathy is the second largest inference of blindness in the US and Europe. Most cases of the visual impairment from diabetic retinopathy can be suppressed in early diagnosis or screening.

(b) Preprocessing

The initial phase in this work is to resize the image to 576×720 and to remove the optic disk. Fundus image is a RGB image which comprise of three channels (red, green, and blue). The green channel segment of the retina image gives the best outcome in the differentiation of veins (darker veins on a brilliant background) as shown in Fig.2. Thus, the green channel of the image is utilized.

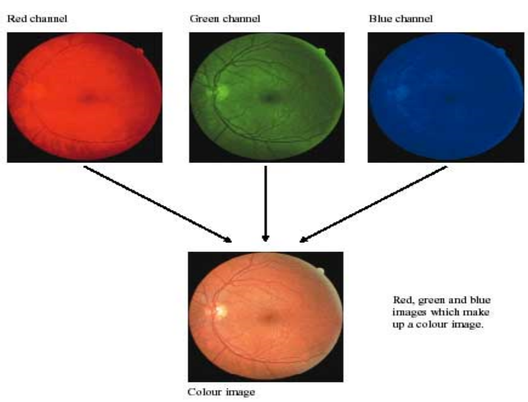

Fig.2 Red, Green, Blue channel of a retinal image

This pre-processing method involves the removal of noise and smoothing the image for further process. The most common noise present in image is the impulse noise which can be removed by median filter. Then the noise filtered image is enhanced for better clarity. The contrast enhancement is done by using the histogram equalization. Canny edge detection technique is utilized for this venture as it is better contrasted with the other comparative MatLab works by having two unique thresholds to identify the edges.

3. SEGMENTATION

Morphological operations are an arrangement of image processing [21-24] operations that resolves the shapes inside the image. It applies an organizing component to the image and yields the image of a similar size. The output estimation of every pixel is determined by the neighboring pixels with its adjacent pixel of input image. The size and shape of the organizing component influences the quantity of pixels being included or expelled from the object in the image.

The most fundamental morphological operations utilized are dilation and erosion. Erosion expels pixels on the protest limits in the picture by transforming it to the background pixel. Dilation, on the other hand, adds pixels to the object limits by changing the background pixel encompassing it. This amplifies the object and different objects could combine as one as shown in Fig.3.

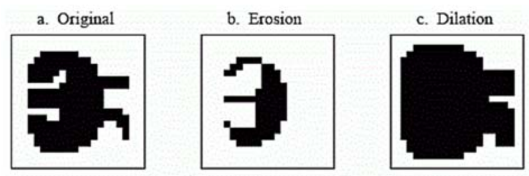

Fig.3 Erosion and Dilation of image

In order to classify the images, different features of fundus images are extracted. They are Exudates, Blood Vessels, Microaneurysms, Homogenity and Texture as shown in flow chart Fig.4.

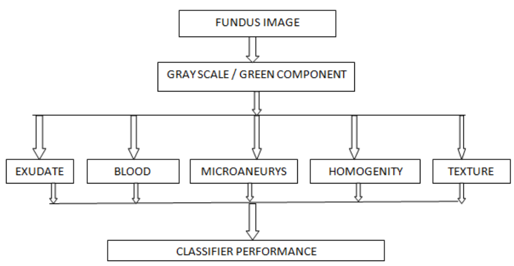

Fig.4 Flow chart of Proposed Method

(a) Exudates Segmentation

Exudates show up as bright yellow-white feature on the retinal layer. Their shape and size change with diverse phases of retinopathy. At first separated green channel image is changed over into grayscale image and afterward preprocessed for consistency. At that point morphological closing operation is completed to evacuate the blood vessels. Morphological closing comprises of erosion followed by dilation.

The canny edge locator is utilized to identify the edges. Canny edge locator is an edge identifying operator that utilizes multistage operations to distinguish extensive variety of edges in image. Solid and feeble fine veins can be distinguished utilizing this Canny edge detection.

The green channel image finds the edges using canny technique; before expelling the circular border to fill the enclosed region. Being the bright spots on the image, adaptive histogram is performed twice after image segmentation to extract the exudates. Acquired bright elements are then compared and removed from large circular border utilizing AND function as shown in Fig.5. The exudates detection algorithm is detailed in Table 1.

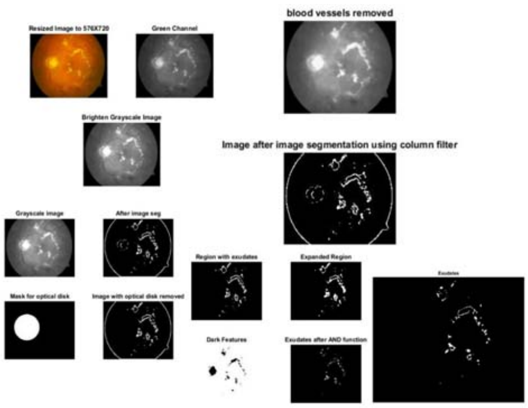

Fig.5 Extracted Exudates region

Table 2
Exudate Segmentation Algorithm

INPUT: Green channel retinal fundus image	
OUTPUT: Exudate segmented image	
Step 1	Read, Resize and Green channel
Step 2	Morphological operation to remove blood vessels
Step 3	Column neighborhood operation
Step 4	Applied Canny edge detection
Step 5	Choosing a Region of Interest
Step 6	Remove optical disk and border
Step7	Morphological erosion to extract exudates
Step8	Area of Exudates

(b) Lood Vessels Segmentation

The border is then recognized and disk element is made with morphological opening operation (erosion & dilation). The eroded image is subtracted with the obtained image and the boundary is acquired.

Adaptive histogram equalization is performed to enhance the contrast of the image and to adjust uneven brightening. A morphological opening operation is performed to highlight the veins. The image is changed over from grayscale to binary by performing thresholding with estimation of 0.1. Median filtering is performed to expel "salt and pepper" noise.

The boundary is acquired by subtracting the border with disk shape. The border is then removed with subsequent to filling the holes that don't touch the edge to acquire the final image (Fig. 6). The pixel estimations of the image are reversed to get just the blood vessels with dark background. Table 2 depicts the blood vessel algorithm.

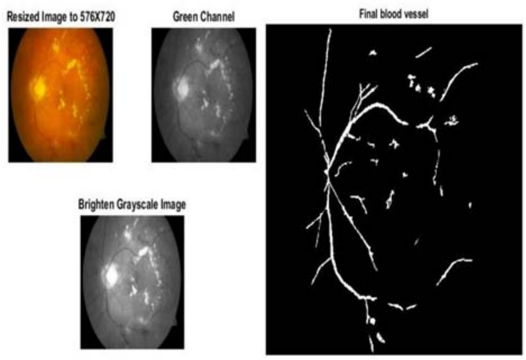

Fig.6 Extracted Blood Vessels

Table 3
Blood vessel segmentation algorithm

INPUT: Green channel retinal fundus image	
OUTPUT: Blood Vessels segmented image	
Step 1	Read, Resize and Green channel
Step 2	Applied Canny edge detection
Step 3	Choosing a Region of Interest
Step 4	Remove optical disk and border
Step 5	Adaptive Histogram to detect blood vessels
Step 6	Morphological operation to extract blood vessels
Step7	Area of Blood Vessels

(c) Icroaneurysms Segmentation

Pre-processing is done to enhance the nature of the image for detection. The pre-preparing technique includes the elimination of noise and smoothing the image for further process. The most well-known noise exhibit in image is the impulsive noise which can be eliminated by median filter.

The red lesions from the fundus image must be portioned to separate the feature elements using morphological operation and thresholding technique (Table 3). The sectioned image is shown in Fig. 7.

The erosion is computed as f(-)k to give a new binary image, where 'g' is the binary image and 'k' is the structuring element. Similarly, dilation is computed as h(+)k. The iterative erosion and dilation and its probability is given as,

$$f(-)k_2 = (f(-)k_2)(-)k_2$$

$$A(-)B = \cup_{n \in B} A_{-n}$$

$$f(+)k_2 = (f(\mp)k_2)(+)k_2$$

$$A(+)B = \cup_{n \in N} A_n$$

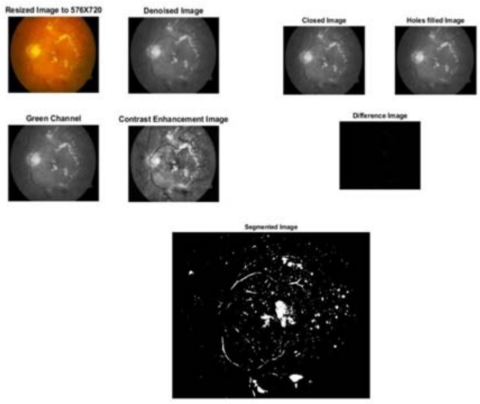

Fig.7 Extracted Microaneurysms

Table 4
Microaneurysms Segmentation Algorithm

INPUT: Green channel retinal fundus image	
OUTPUT: Microaneurysm segmented image	
Step 1	Read, Resize and Green channel
Step 2	Noise removal by Median Filter
Step 3	Contrast enhancement by Adaptive histogram
Step 4	Morphological operation(erosion & dilation)
Step 5	Thresholding to extract Microaneurysms
Step6	Area of Microaneurysms

4. FEATURE EXTRACTION

(a) Area

An area graph explains the elements in Y as curves. It covers the area beneath every curve. When Y is a matrix, the curves are arranged by showing the relative condition for each row element to the exact height of the curve in each x interval. It is otherwise described as the total number if pixel value '1' in the binary image

(b) Omogenity

Grey Level Co-occurrence Matrix (GLCM) is the calculation of the occurrence of every pixel match happening for various blends of pixel brightness values in a image. The function "graycomatrix" is utilized to make the GLCM of the grayscale image. It ascertains how frequently the pixel with value i is the gray level. Every component in the GLCM shows the frequent occurrence.

The function "graycoprops" standardizes the GLCM so that the sum of its components is equivalent to 1. Homogeneity is the estimation of the closeness of the distribution of components in the GLCM to the GLCM diagonal to returns a value in-between 0 and 1. The homogeneity formula is,

$$\sum_{m,n} \frac{h(m,n)}{1+|m-n|}$$

(c) Texture

Entropy is the statistical measure of the arbitrariness of the grayscale image's texture. It is a texture examination function in the MATLAB Image Processing Toolbox. The green segment of the image is connected with adaptive histogram equalization twice for enlightenment of texture. The function "entropy" is then utilized on the image which gives back a scalar value. This exhibits the entropy of intensity of image.

5. CLASSIFICATION

5.1 Neural Network

Two types of Neural Network Classifier (NN) is utilized. They are feed-forward back propagation network and k-Nearest Neighbour Network.

(a) Feed Forward Neural Network

They are used to manage the neural system. Regulated learning is by supervising the NN with input information and matches them with outcomes shown in Table 4. Its weights would change as indicated by its learning rules as it experiences tested before being tried for accuracy. The images with its response are trained into neural system and their executions are analyzed for diaretdb, Messidor and ROC databases.

(b) k- nearest neighbour (knn)

K Nearest Neighbor (KNN) is one of those algorithms that are extremely easy to figure out and is adaptable. KNN does not utilize the trained data points to do any speculation. This implies the training phase is entirely quick. The data can be scalars or perhaps even multidimensional vectors. Since the points are in component space, they have a separation. Each of the training data comprises of an arrangement of vectors and class label related with every vector. A single number "k" is chosen which decides the number of neighbors that impacts the classification. This is normally an odd number if the number of classes is 2. In the event that k=1, then the algorithm is simply called the nearest neighbor algorithm.

5.2 Decision Tree

Decision Trees (DTs) are a non-parametric managed learning strategy utilized for classification and regression. The objective is to make a model that predicts the estimation of a target by using simple decision rules derived from the data features. A decision tree is a diagram that uses an expanding technique to show each conceivable result of a choice. The decision trees can be drawn by hand or made with a design program or concentrated programming. Casually, decision trees are helpful for centering exchange when a gathering must settle on a choice. Automatically, they can be utilized to allocate time or different qualities to conceivable results with the goal that choices can be computerized. Decision tree programming is utilized as a part of information mining to improve complex key difficulties and assess the cost-viability of research and business choices. Factors in a decision tree are generally exhibited by circles.

The ROC curve is a principle tool for symptomatic test assessment. In a ROC curve the true positive rate (Sensitivity) is plotted as a function of the false positive rate (100-Specificity) for various cut-off point. Each point on the ROC curve represents a sensitivity/specificity pair relating to a specific decision threshold. The area under the ROC curve (AUC) is a measure of how well a parameter can recognize between two diagnostic groups (sick/typical).

On the other hand conceivable cut-off point is selected to differentiate between the two populations. There will be some cases with the sickness accurately named as positive (TP = True Positive fraction), but few cases with the ailment will be ordered negative (FN = False Negative fraction). Then again, some cases without the disease will be correctly classified as negative (TN = True Negative fraction), but some cases without the sickness will be named as positive (FP = False Positive fraction).

A scatterplot is regularly utilized to recognize potential relationship between two factors, where one might be thought to be an illustrative variable and another may be considered a reaction variable. A positive relationship between instruction and response would be indicated on a scatterplot by a upward pattern (positive slope). A negative affiliation would be demonstrated by the inverse impact (negative slope).

5.3 Support Vector Machine

“Support Vector Machine” (SVM) is a supervised machine learning algorithm which can be utilized for both classification and regression challenges. Support Vector Machines are based on the idea of decision planes that define decision boundaries. Support Vector Machine (SVM) is fundamentally a classifier technique that performs classification tasks by developing hyper planes in a multidimensional space that distinct case of different class labels. For all categorical variables a dummy variable is assigned with case values as either 0 or 1.

6. SIMULATION RESULTS

To inspect the efficacy of the proposed work the complete algorithm was carried by the datasets and results of exudates, blood vessels and microaneurysms detection which were gathered. The time taken for execution is 10 seconds with PC of Intel i3 processor and 2GB RAM.

The tool used is MATLAB R2016a with three databases shown in Table 1. The classification depends on how the extracted features are trained into the classifiers and how the test is directed. The proposed work utilizes four sorts of classifiers to demonstrate their execution under different databases.

(a) Feed Forward Neural Network

Table 5
Details of feed forward neural network for databases

NEURAL NETWORK	diaretdb	Messidor	ROC
Input samples	50	100	89
Output samples	1		1
Training sets	20	65	32
Validation sets	22	25	13
Testing sets	9	10	5
Hidden layer	20	20	10

The confusion matrix is analyzed by its true positive (TP), true negative (TN), false positive (FP) and false negative (FN) of the trained image. The true positive rate is the accuracy of the network and 1- false negative produce the sensitivity of the neural network. The ROC curve is plotted using TN, TP, FN, FP values to show the performance of the neural network. For the neural network with good performance characteristics the ROC curve should be 90° elevated.

The training state graph shows the values which are validated as false value and true values. The values which are predicted as false are plotted above and true values which are predicted are plotted in the axis line of the graph. The performance graph shows the cross entropy values calculated for trained set; validations set and test data set. The test data set should be plotted on the line of best curve. It should have at least one value as same as the best curve. The trained set will always differ from the validation curve the set details shown in table 5.

The error histogram shows the error graph of the data set utilized for testing. The high value shows the error point during testing. The zero error line is with higher instance value. The error value is actually calculated by the difference of output and the target.

(b) Knn Classifier
Each of the training data comprises of an arrangement of vectors and class label related with every vector. A single number "k" is chosen which decides the number of neighbors that impacts the classification. This is normally an odd number if the number of classes is 2. In the event that k=1, then the algorithm is simply called the nearest neighbor algorithm.

(c) Decision tree classifier

Table 6
Dataset details for Decision Tree and SVM

	Diaretdb	Messidor	ROC
Input samples	89	100	50
Predicted features	5	5	5
Response values	1/0	1/0	1/0

The ROC curve is a principle tool for symptomatic test assessment. In a ROC curve the true positive rate (Sensitivity) is plotted as a function of the false positive rate (100-Specificity) for various cut-off point. Each point on the ROC curve represents a sensitivity/specificity pair relating to a specific decision threshold. The area under the ROC curve (AUC) is a measure of how well a parameter can recognize between two diagnostic groups (sick/typical).

On the other hand conceivable cut-off point is selected to differentiate between the two populations. There will be some cases with the sickness accurately named as positive (TP = True Positive fraction), but few cases with the ailment will be ordered negative (FN = False Negative fraction). Then again, some cases without the disease will be correctly classified as negative (TN = True Negative fraction), but some cases without the sickness will be named as positive (FP = False Positive fraction).

A scatterplot is regularly utilized to recognize potential relationship between two factors, where one might be thought to be an illustrative variable and another may be considered a reaction variable. A positive relationship between instruction and response would be indicated on a scatterplot by a upward pattern (positive slope). A negative affiliation would be demonstrated by the inverse impact (negative slope).

(d) Support Vector Machine

Support Vector Machine (SVM) is fundamentally a classifier technique that performs classification tasks by developing hyper planes in a multidimensional space that distinct case of different class labels. For all categorical variables a dummy variable is assigned with case values as either 0 or 1.

7. ACCURACY COMPARISON

Table 7
Accuracy Comparisons of Classifiers

DATABASE / CLASSIFIERS	DIARETDB	MESSIDOR	ROC
NEURAL NETWORK	98%	98%	98%
DECISION TREE	98%	98%	95%
K-NEAREST NEIGHBOR	73.43%	72.16%	86.8%
LINEAR SVM	91%	95%	95%
GAUSSIAN SVM	70.8%	74.6%	89.3%

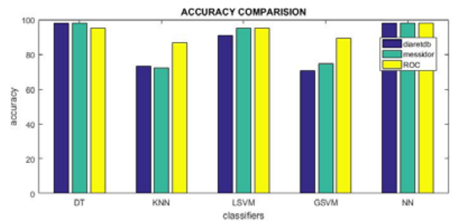

Fig. 8 Accuracy comparison

From Table 7 and Fig 8 it is clear that the accuracy range is best in neural network classifier followed by decision tree classifier. The linear support vector machine shows better results compared to the k- nearest neighbor and Gaussian support vector machine. Moreover the database ROC shows constant range in all type of classifiers, whereas the diaretdb database shows vast change in the range of accuracy for every classifier.

8. CONCLUSION

The fundus images from database are used to extract the features such as exudates, microaneurysms, blood vessels, homogeneity and texture. Based on the value of each feature which was isolated is been used to grade the disease condition. The set of images from the database are trained into each classifier to analyze its performance. The performances are analyzed using the confusion matrix, roc curve and performance graphs. Based on this performance the accuracy of each classifier is compared. The comparison shows that the Neural Network classifier excels the other types of classifiers, closely followed by the Decision Tree classifier for diabetic retinopathy recognition.

REFERENCES

[1] M. D. Abramoff, J. M. Reinhardt, S. R. Russell, J. C. Folk, V. B. Mahajan, M. Niemeijer, and G. Quellec, “Automated early detection of diabetic retinopathy,” Ophthalmology, no. 6, pp.1147–1154, Apr 2006.

[2] O. Faust, R. AcharyaU, E. Y. K. Ng,K.-H. Ng, and J. S. Suri, “Algorithms for the automated detection of diabetic retinopathy using digital fundus images: A review J. Med. Syst., Apr 2008.

[3] World Health Organization. (2012, Sep.).“Diabetes programme,” [Online]. Available: http://www.who.int/diabetes/en

[4] N. Younis, D. M. Broadbent, S. P. Harding, and J. R. Vora, “Prevalence of diabetic eye disease in patients entering a systematic primary care-based eye screening programme,” Diabet. Med., vol. 19, pp. 1014–1021, 2002.

[5] H. Taylor, J. Xie, S. Fox, R. Dunn, A. Arnold, and J. Keeffe, “The prevalence and causes of vision loss in indigenous australians: The national indigenous eye health survey,” Med J. Aust., vol. 192, no. 6, pp. 312–318, 2010.

[6] D. J. Pettitt, A. Okada Wollitzer, L. Jovanovic, G. He, and E. Ipp, “Decreasing the risk of diabetic retinopathy in a study of case management: The california medical type 2 diabetes study,” Diabetes Care, vol. 28, pp. 2819–2822, 2005.

[7] Q. Mohamed, M. C. Gillies, and T. Y. Wong, ―Management of diabetic retinopathy: A systematic review,” J. Amer. Med. Assoc., vol. 298, no. 8, pp. 902–916, 2007.

[8] M. James, D. A. Turner, D. M. Broadbent, J. Vora, and S. P. Harding, “Cost effectiveness analysis of screening for sight threatening diabetic eye disease,” Br. Med. J., vol. 320, pp. 1627–1631, 2000.

[9] L. Giancardo, F. Meriaudeau, T. Karnowski, Y. Li, K. Tobin, and E. Chaum, “Microaneurysm detection with radon transform-based classification on retina images,” in Proc. Intl. Conf. IEEE Eng. Med. Biol. Soc., 2011, pp. 5939–5942.

[10] B. Antal, I. Lazar, A. Hajdu, Z. Torok, A. Csutak, and T. Peto “Evaluation of the grading performance of an ensemble-based microaneurysm detector,” in Proc. Intl. Conf. IEEE Eng. Med Biol. Soc., 2011, pp. 5943–5946.

[11] A. D. Fleming, S. Philip, K. A. Goatman, J. A. Olson, and P. F. Sharp, ―Automated microaneurysm detection using local contrast normalization and local vessel detection,” IEEE Trans. Med. Imag., vol. 25, no. 9, pp. 1223–1232, 2006.

[12] M. Niemeijer, M. D. Abràmoff, and B. van Ginneken, “Image structure clustering for image quality verification of color retina images in diabetic retinopathy screening,” Med. Image Anal. 10(6), 888–98 (2006).

[13] J. M. Pires Dias, C. M. Oliveira, and L. A. da Silva Cruz, “Retinal image quality assessment using generic image quality indicators,” Inf. Fusion 19, 73–90 (2014).

[14] A. D. Fleming et al., “Automated clarity assessment of retinal images using regionally based structural and statistical measures,” Med. Eng. Phys. 34(7), 849–859 (2012).

[15] L. Giancardo and F. Meriaudeau, “Quality assessment of retinal fundus images using elliptical local vessel density,” in New Developments in Biomedical Engineering, D. Campolo, Ed. (2010).

[16] H. Yu, C. Agurto, and S. Barriga, “Automated image quality evaluation of retinal fundus photographs in diabetic retinopathy screening,”in IEEE Southwest Symposium on Proc. of Image Analysis and Interpretation (SSIAI), pp. 125–128, IEEE, Santa Fe, New Mexico (2012).

[17] Akara SK., Bunyarit U, Sarah B, Williamson TH. Automatic detection of diabetic retinopathy exudates from non-dilated retinal images using mathematical morphology methods. Comput Med Imaging Graph. Elsevier Journal. 2008; 32: 720–727

[18] J. Saito, D. Roxburgh, D. Sutton, and A. Ellingford, “A new method of image analysis of fluorescein angiography applied to age-related macular degeneration,” Eye, vol. 9, pp. 70–76, 1995.

[19] E. Trucco, C. R. Buchanan, T. Aslam, and B. Dhillon, “Contextual detection of ischemic regions in ultra-wide-field-of-view retinal fluorescein angiograms,” in Proc. IEEE EMBC, 2007, pp. 6739–6742.

[20] C. L. Tsai, C. L. Yang, S. J. Chen, C. H. Lin, K. S. Chan, and W. Y. Lin, “Automatic characterization of classic choroidal neovascularization by using

adaboost for supervised learning," Invest. Ophthalmol. Vis. Sci., vol. 52, pp. 2767–2774, 2011.

[21] Syamala, M., Nalini, N.J., Ragupathy, R., Magulur, L.P., "Random forest classifier approach for blurred images", (2017) International Journal of Pure and Applied Mathematics, 116 (6 Special Issue), pp. 67-72.

[22] Utkam, S.G., Parasa, R., Kondapaneni, A., Tulabandula, P.R.K., Kuppala, D.R., "A secured symmetric key encryption technique using images as secret keys", (2017) International Journal of Pure and Applied Mathematics, 116 (6 Special Issue), pp. 149-153.

[23] Veeraiah, T., Mahamkali, A., Kishore, B.N.P., Rao, A.N., Rao, S.K.M., "Image denoising by profunditymap methodusing diagram base change and group scanty", (2017) International Journal of Pure and Applied Mathematics, 115 (8 Special Issue), pp. 143-149.

[24] Veeraiah, T., Rao, S.K.M., "Classification of fuzzy rule based order-statistic filters for color images", (2017) International Journal of Pure and Applied Mathematics, 115 (8 Special Issue), pp. 189-194.